Statistica Sinica Preprint No: SS-2025-0204	
Title	Frequency Domain Resampling for Gridded Spatial Data
Manuscript ID	SS-2025-0204
URL	http://www.stat.sinica.edu.tw/statistica/
DOI	10.5705/ss.202025.0204
Complete List of Authors	Souvick Bera, Daniel Nordman and Soutir Bandyopadhyay
Corresponding Authors	Soutir Bandyopadhyay
E-mails	bsoutir@gmail.com
Notice: Accepted author version.	

Frequency Domain Resampling for Gridded Spatial Data

Souvick Bera[1], Daniel J. Nordman[2] and Soutir Bandyopadhyay[1]

[1] *Colorado School of Mines and* [2] *Iowa State University*

Abstract:

In frequency domain analysis for spatial data, spectral averages based on the periodogram often play an important role in understanding spatial covariance structure, but also have complicated sampling distributions due to complex variances from aggregated periodograms. In order to non-parametrically approximate these sampling distributions for purposes of inference, resampling can be useful, but previous developments in spatial bootstrap have faced challenges in the scope of their validity, specifically due to issues in capturing the complex variances of spatial spectral averages. As a consequence, existing frequency domain bootstraps for spatial data are highly restricted in application to only special processes (e.g. Gaussian) or certain spatial statistics. To address this limitation and to approximate a wide range of spatial spectral averages, we propose a practical hybrid-resampling approach that combines two different resampling techniques in the forms of spatial subsampling and spatial bootstrap. Subsampling helps to capture the variance of spectral averages while bootstrap captures the distributional shape. The hybrid resampling procedure can then accurately quantify uncertainty in spectral inference under mild spatial assumptions. Moreover, compared to the more studied time series setting, this work fills a gap in the theory of subsampling/bootstrap for spatial data regarding spectral average statistics.

Key words and phrases: Spatial Frequency Domain Bootstrap, Spectral Mean, Periodogram.

1. Introduction

In recent years, there has been a marked increase in research on the analysis of spatial data using the frequency domain approach (see, for example, Bandyopadhyay et al., 2017; Bandyopadhyay and Lahiri, 2010; Bandyopadhyay et al., 2015; Bandyopadhyay and Rao, 2016; Fuentes, 2006, 2007; Hall et al., 1994; Im et al., 2007; Matsuda and Yajima, 2009; Van Hala et al., 2017, 2020). As a benefit, analysis in the frequency domain allows inference about covariance structures through a data transformation (i.e., a Fourier or periodogram-based transform), without the need for a full probability model for spatial data. Resampling methods, such as subsampling and bootstrap, for spatial data have gained popularity in recent decades because these approaches can often allow for uncertainty quantification and distributional approximations for complicated spatial statistics in an nonparametric or model-free fashion; see Davison and Hinkley (1997), Sherman and Carlstein (1994) and Sherman (1998). In a recent study, Ng et al. (2021) introduced a type of frequency domain bootstrap (FDB) for Gaussian spatial data on grid. Although this work offers a significant contribution to nonparametric spatial approximations, the resampling methodology comes with certain hard limitations in application. Firstly, the FDB of Ng et al. (2021) is generally not valid for approximating many spatial spectral averages of interest, because the latter have complex variance structures that this FDB proposal cannot correctly estimate. In particular, the challenge is that spectral mean statistics have variances that depend both on spatial covariances as well as higher order (i.e., fourth) process cumulants, which arise due to covariances between the spatial periodogram ordinates. Technically, it is the variance contributions related to higher order cumulants that are generally missed or ignored in the FDB approach of Ng et al. (2021), unless the spatial data are Gaussian (i.e., so that these variance components become zero). Consequently and secondly, the spatial bootstrap results of Ng et al. (2021) are established under assumptions of Gaussianity, which can be stringent and may not suitably reflect the distributional nature of spectral average statistics in general practice. These aspects motivate a need to modify the spatial FDB of Ng et al. (2021) to handle a broader range of spectral statistics with application potentially *non-Gaussian* spatial processes.

To provide improved and more universally valid distributional approximations with spatial spectral statistics, we introduce a resampling technique called spatial *Hybrid Frequency Domain Bootstrap* (HFDB) which aims to merge two different resampling schemes in the forms of subsampling and bootstrap into one overall approach in the frequency domain. The idea that spatial subsampling can be used to correctly estimate the variances of complicated spectral averages, while bootstrap can be used to re-create the shape of the sampling distributions. Essentially then, subsampling plays a role in appropriately modifying the spreads of FDB distributional approximations, where this bootstrap would otherwise be invalid without such scaling adjustments. The advantage of the proposed HFDB method is that this can accurately capture the uncertainty in spatial spectral statistics for calibrating tests or confidence intervals without requiring stringent conditions on the spatial processes or assumptions of Gaussianity; in particular, the conditions needed to validate HFDB basically amount to mild assumptions for ensuring that spectral averages have limit distributions at all. This work then intends to close some gaps in the scope of applying resampling approximations for spatial data, which is practically valuable. Additionally, our work also bridges some gaps in the theory of subsampling and bootstrap for spatial data, and extends some recent theoretical findings for spectral inference with time series to the spatial data setting.

We conclude this section by briefly overviewing FDB for time series and providing connections to the spatial bootstrap here. In time series analysis, FDB has received much attention and interest toward approximating the distributions of spectral statistics derived from the periodogram (cf. Kreiss and Paparoditis, 2012; Kreiss and Lahiri, 2012; Lahiri, 2003b; Politis and McElroy, 2019). The key concept behind this method is to mimic a type of asymptotic independence that exists in the periodogram in order to generate versions of periodogram ordinates in the bootstrap world by independent resampling (cf. Dahlhaus and Janas, 1996; Jentsch and Kreiss, 2010; Kreiss and Paparoditis, 2003, 2012, 2023; Kreiss et al., 2011). In the last three decades, there has been a progression of FDB methods, often relying on specific assumptions about the underlying time series (e.g., linear process) or differing cases of spectral mean parameters. Recently, a major advancement was achieved by Meyer et al. (2020) who introduced an innovative bootstrap method, called the hybrid periodogram bootstrap (HPB), that represents the state-of-the-art approach for time series inference concerning spectral means. Related to this, Yu et al. (2023) recently studied subsampling for use in conjunction with HPB, where subsampling helps to justify the latter bootstrap approach under weaker assumptions than Meyer et al. (2020) and so HPB extends to a wide range of application with various time processes. Unlike bootstraps that aim to re-create statistics at the same data level as the original sample, subsampling is a different resampling approach that generates smaller-scale copies of statistic; because of this distinction, subsampling often applies under weaker conditions than bootstrap, though bootstrap can provide more accurate distributional approximations when valid (cf. Politis et al., 1999). The spatial FDB proposed by Ng et al. (2021) is the spatial equivalent of one of the original FBD methods for time series (cf. Dahlhaus and Janas, 1996; Jentsch and Kreiss, 2010;

Kreiss and Paparoditis, 2003), while the proposed spatial HFDB here intends to be a spatial analog of the HPB for time series as studied in Meyer et al. (2020) when combined with a subsampling extension as in Yu et al. (2023). This development is non-trivial for spatial data and, similar to the time series setting, is crucial for avoiding restrictive process and moment conditions for dependent data. Finally, it is worth mentioning that, similar to Ng et al. (2021), we focus our resampling presentation on spatial observations lying on a lattice in two-dimensional space, though findings can be extended to gridded data in more general spatial sampling dimensions $d \geq 2$.

The remainder of the paper is organized as follows. Section 2 introduces the distributions of spectral mean statistics, which form the basis for inference, along with the associated framework. Section 3 presents a spatial subsampling framework in the frequency domain and establishes its consistency, forming the foundation for the proposed bootstrap procedure. A detailed discussion of the hybrid bootstrap method for spatial data is provided in Section 4. Section 5 presents numerical studies to evaluate the accuracy of the proposed procedure across several inference problems. Finally, Section 6 concludes. Additional technical details and simulation results can be found in Appendix and Supplementary Materials, respectively.

2. Distributions of Spectral Mean Statistics

2.1 Spatial process and sampling design

Throughout this paper, we follow spatial sampling framework similar to Bandyopadhyay and Lahiri (2010) and Ng et al. (2021). Let $\{Z(\mathbf{s})\} : \mathbf{s} \in \mathbb{Z}^2\}$ denote a real-valued second-order stationary process located on a regular integer grid $\mathbb{Z}^2$. In this fashion, potential observations lie on a spatial lattice with a constant separation in each coordinate direction (which we take to be 1 though other scaling is possible as well). We assume that the random process $Z(\mathbf{s})$ is observed at $n \equiv n_1 n_2$ sampling sites defined by

$$\{\mathbf{s}_1, \ldots, \mathbf{s}_n\} \equiv \{\mathbf{s} \in \mathbb{Z}^2 : \mathbf{s} \in \mathcal{D}_n\} = \mathcal{D}_n \cap \mathbb{Z}^2$$

given by those locations on the grid $\mathbb{Z}^2$ that lie within a rectangular sampling region $\mathcal{D}_n \equiv [1, n_1] \times [1, n_2]$ for integers $n_1, n_2 \geq 1$. For spatial data analysis, the above sampling framework corresponds to a so-called pure increasing domain for developing spatial results (cf. Cressie, 1993). That is, in this scheme, more spatial observations are available (i.e., $n \to \infty$) as spatial sampling region expands in size in each direction (i.e., $n_i \to \infty$ for $i = 1, 2$).

2.2 Spectral mean parameters

Suppose that the second order stationary spatial process $\{Z(\mathbf{s}) : \mathbf{s} \in \mathbb{Z}^2\}$ has a spectral density denoted as $f(\boldsymbol{\omega}) : \Pi^2 \longrightarrow [0, \infty)$ where $f(\boldsymbol{\omega}) \equiv (2\pi)^{-2} \sum_{\mathbf{h} \in \mathbb{Z}^2} \mathrm{Cov}(Z(\mathbf{0}), Z(\mathbf{h})) \exp(-\iota \mathbf{h}^\top \boldsymbol{\omega})$, for $\iota \equiv \sqrt{-1}$ and for $\boldsymbol{\omega} \in \Pi^2 \equiv [-\pi, \pi]^2$. Then, the target spatial parameter for inference is a *spectral mean* parameter defined as an integral

$$M(\psi) \equiv \int_{\Pi^2} \psi(\boldsymbol{\omega}) f(\boldsymbol{\omega}) d\boldsymbol{\omega}, \tag{2.1}$$

involving f and some chosen/given function $\psi : \Pi^2 \longrightarrow \mathbb{R}$ of bounded variation. Spectral mean parameters are common in the spatial data analysis for studying the spatial covariance structure of the data with an unknown distribution. Such quantities have a well-established history for both time series and spatial data (cf. Politis and McElroy, 2019, for details), dating as far back as Parzen (1957), and many spatial parameters of interest can be expressed in the form of a spectral mean. Standard examples of spectral means include auto-covariances and spectral distributions, as described below, depending on the choice of ψ above.

Next we give some examples of spectral mean parameters arising in frequency domain analysis (cf. Bandyopadhyay et al., 2015; Dahlhaus, 1985; Dahlhaus and Janas, 1996; Parzen, 1957; Subba Rao, 2018; Van Hala et al., 2017, 2020 and the references therein).

Examples of spectral mean parameters

1. Covariance function. For a lag vector $\mathbf{h} \in \mathbb{Z}^2$, if we consider the function $\psi(\boldsymbol{\omega}) = \cos(\mathbf{h}^\top \boldsymbol{\omega})$ in 2.1, this leads to the autocovariance function $\gamma(\mathbf{h}) \equiv \mathrm{Cov}(Z(\mathbf{0}), Z(\mathbf{h}))$, which can be viewed as a spectral mean $M(\psi)$. Note that, for testing the special hypothesis $H_0 : Z(\mathbf{s})$ is white noise (constant f), a test based on the process auto-covariances can be applied, similar to some Portmanteau tests (cf. Li and McLeod, 1986; Ljung and Box, 1978) using the fact that the spectral means $M(\psi)$ are zero under this H_0 for the function choice $\psi(\boldsymbol{\omega}) = [\cos(\mathbf{h}_1{}^\top \boldsymbol{\omega}), \ldots, (\cos(\mathbf{h}_k{}^\top \boldsymbol{\omega})]^\top$ for some integer lags $\mathbf{h}_1, \ldots, \mathbf{h}_k$.

2. Spectral distribution function. For a vector $\mathbf{t} \in \mathbb{R}^2$, the spectral distribution function is defined as $F(\mathbf{t}) \equiv \int_{\mathbb{R}^2} \mathbb{I}_{(-\infty,\mathbf{t}]}(\boldsymbol{\omega}) f(\boldsymbol{\omega}) d\boldsymbol{\omega}$, which corresponds to a spectral mean parameter defined by $\psi(\boldsymbol{\omega}) = \mathbb{I}_{(-\infty,\mathbf{t}]}(\boldsymbol{\omega})$ in (2.1) where $\mathbb{I}(\cdot)$ is the indicator function and $(-\infty, \mathbf{t}] \equiv (-\infty, t_1] \times (-\infty, t_2]$. The spectral distribution function plays a role in determining the smoothness of the sample paths of the spatial process $Z(\cdot)$ (cf. Stein, 1999).

3. Assessment of spatial covariance structures. When analyzing spatial data, it can be useful to assess the spatial covariance structures in a nonparametric manner, without requiring specific distributional assumptions about the data. General testing methods can be developed of evaluating different hypotheses about spatial covariances, such as tests of isotropy or separability, by examining $M(\psi)$ with appropriate choices of $\psi(\boldsymbol{\omega})$ functions. For more details, refer to Van Hala et al. (2017, 2020).

4. Whittle Estimation. Suppose $\{f_\theta\}$ represents a parametric family of spectral densities (indexed by θ). Whittle estimation aims to identify the closest member f_θ to the true density f (cf. Taniguchi, 1979). Assuming real-valued θ for illustration, the solution to a spectral mean $M(\psi) = 0$ identifies the appropriate f_θ under certain conditions, using a function $\psi(\boldsymbol{\omega}) = [1 - f_\theta(\boldsymbol{\omega})/f(\boldsymbol{\omega})] \frac{d}{d\theta} f_\theta^{-1}(\boldsymbol{\omega}), \boldsymbol{\omega} \in \mathbb{R}^2$, defined by the derivative of $f_\theta^{-1}(\boldsymbol{\omega}) \equiv 1/f_\theta(\boldsymbol{\omega})$.

5. Goodness-of-fit tests. There has been increasing interest in frequency domain based tests to assess model adequacy (cf. Crujeiras and Fernandez-Casal, 2010; Van Hala et al., 2020; Weller and Hoeting, 2020). Consider a test involving a simple null hypothesis $H_0 : f = f_0$ against an alternative $H_0 : f \neq f_0$ for some candidate spectral density f_0. One immediate test for H_0 is based on the function $\psi(\boldsymbol{\omega}) = 1/f_0(\boldsymbol{\omega})$ with $M(\psi)$ a constant under this simple H_0. To test the composite hypothesis $H_0 : f \in \mathcal{F}$ for a specified parametric class $\mathcal{F}$, several frequency domain tests have been proposed in time series (cf. Beran, 1992, Milhøj, 1981, Paparoditis, 2000, Nordman and Lahiri, 2006). These tests can use Whittle estimation to choose the "best" fitting model from $\mathcal{F}$ and then compare the fitted density to the periodogram across all ordinates. One can adapt strategies for goodness-of-fit tests with time series (cf. Nordman and Lahiri, 2006), which combine aspects of model fitting and model comparison into a choice of estimating function ψ, to spatial processes.

6. Variogram model fitting. A popular approach to fitting a parametric variogram model to spatial data is through the method of least squares; see Cressie (1993). Let $\{2\nu(\cdot;\theta) : \theta \in \Theta\}$, $\Theta \subset \mathbb{R}^p$ denote a class of valid variogram models for the true variogram $2\nu(\mathbf{h}) \equiv \mathrm{Var}(Z(\mathbf{h}) - Z(\mathbf{0}))$, $\mathbf{h} \in \mathbb{Z}^2$ of the spatial process. Let $2\widehat{\nu}_n(\mathbf{h})$ denote the sample variogram at lag $\mathbf{h}$ based on $Z(\mathbf{s}_1), \ldots, Z(\mathbf{s}_n)$ (cf. Chapter 2, Cressie, 1993). Then one can fit the variogram model by estimating the parameter θ that minimizes the criterion: $\widehat{\theta}_n \equiv$

$\mathrm{argmin}\Big\{ \sum_{i=1}^m \Big(2\widehat{\nu}_n(\mathbf{h}_i) - 2\nu(\mathbf{h}_i;\theta)\Big)^2 : \theta \in \Theta\Big\}$ for a given set of lags $\mathbf{h}_1, \ldots, \mathbf{h}_m$. Expressing the variogram in terms of the spectral density function, we get an equivalent spectral estimating equation for identifying θ: $M(\psi) = 0$ for

$$M(\psi) \equiv \int_{\mathbb{R}^2} \Big[\sum_{i=1}^m \Big\{1 - \cos(\mathbf{h}_i{}^\top \boldsymbol{\omega}) - \nu(\mathbf{h};\theta)\Big\} \nabla[2\nu(\mathbf{h}_i;\theta)]\Big] f(\boldsymbol{\omega}) d\boldsymbol{\omega},$$

using $\psi_\theta(\boldsymbol{\omega}) = \sum_{i=1}^m \Big\{1 - \cos(\mathbf{h}_i{}^\top \boldsymbol{\omega}) - \nu(\mathbf{h};\theta)\Big\} \nabla[2\nu(\mathbf{h}_i;\theta)]$.

2.3 Spectral mean statistics and sampling distributions

From the spatial process $Z(\cdot)$ observed on the sampling region $\mathcal{D}_n$, where $n = n_1 n_2$ is the number of observations, we define $\mathcal{I}_n(\boldsymbol{\omega})$ to be the periodogram at a frequency $\boldsymbol{\omega} \in \Pi^2$ as

$$\mathcal{I}_n(\boldsymbol{\omega}) \equiv (2\pi)^{-2} n^{-1} \left| \sum_{s_1=1}^{n_1} \sum_{s_2=1}^{n_2} Z(\mathbf{s}) \exp\left(-\iota \mathbf{s}^\top \boldsymbol{\omega}\right) \right|^2, \quad \mathbf{s} \equiv (s_1, s_2)^\top, \text{ where } \iota \equiv \sqrt{-1}.$$

Using $\mathcal{I}_n(\cdot)$ in place of $f(\cdot)$ in (2.1), a standard estimator of the spectral mean parameter $M(\psi)$ is then the *spectral mean statistic*, or *spectral average*, given in Riemann sum form by

$$\widehat{M}_n(\psi) \equiv (2\pi)^2 n^{-1} \sum_{\mathbf{j} \in \mathcal{J}_n} \psi(\boldsymbol{\omega}_{\mathbf{j},n}) \mathcal{I}_n(\boldsymbol{\omega}_{\mathbf{j},n}),$$

using discrete frequencies $\boldsymbol{\omega}_{\mathbf{j},n} \equiv (2\pi j_1/n_1, 2\pi j_2/n_2)$ defined by $\mathbf{j} \equiv (j_1, j_2) \in \mathcal{J}_n$ with index set $\mathcal{J}_n \equiv \{\lfloor -(n_1-1)/2 \rfloor, \ldots, n_1 - \lfloor n_1/2 \rfloor\} \times \{\lfloor -(n_2-1)/2 \rfloor, \ldots, n_2 - \lfloor n_2/2 \rfloor\} \setminus \{(0,0)\}$ denoting the (nonzero) discrete Fourier frequency grid. For calibrating tests and confidence intervals, a spectral mean statistic has a large-sample normal distribution under mild conditions (cf. Brillinger, 2001; Dahlhaus, 1985) given by

$$H_n(\psi) \equiv n^{1/2}\{\widehat{M}_n(\psi) - M(\psi)\} \xrightarrow{D} \mathcal{N}(0, \sigma^2 = \sigma_1^2 + \sigma_2^2) \text{ as } n \to \infty, \tag{2.2}$$

with variance components

$$\begin{aligned}\sigma_1^2 \equiv \sigma_1^2(\psi) &= (2\pi)^2 \int_{\Pi^2} \psi(\boldsymbol{\omega})[\psi(\boldsymbol{\omega}) + \psi(-\boldsymbol{\omega})] f^2(\boldsymbol{\omega})\, d\boldsymbol{\omega}, \\ \sigma_2^2 \equiv \sigma_2^2(\psi) &= (2\pi)^2 \int_{\Pi^2} \int_{\Pi^2} \psi(\boldsymbol{\omega}_1)\psi(\boldsymbol{\omega}_2) f_4(\boldsymbol{\omega}_1, \boldsymbol{\omega}_2, -\boldsymbol{\omega}_2)\, d\boldsymbol{\omega}_1\, d\boldsymbol{\omega}_2\end{aligned}$$

where, for $\boldsymbol{\omega}_1, \boldsymbol{\omega}_2, \boldsymbol{\omega}_3 \in \Pi^2$,

$$f_4(\boldsymbol{\omega}_1, \boldsymbol{\omega}_2, \boldsymbol{\omega}_3) \equiv (2\pi)^{-3} \sum_{\mathbf{h}_1, \mathbf{h}_2, \mathbf{h}_3 \in \mathbb{Z}^2} \mathrm{cum}(Z(\mathbf{0}), Z(\mathbf{h}_1), Z(\mathbf{h}_2), Z(\mathbf{h}_3)) \exp\left(-\iota \sum_{\ell=1}^{3} \mathbf{h}_\ell^\top \boldsymbol{\omega}_\ell\right),$$

denotes the 4th-order cumulant spectral density. Given the complicated structure in the limit distribution from (2.2), one attractive approach is to consider resampling for approximating the distribution of $H_n(\psi)$ nonparametrically. However, estimation of the variance component σ_2^2, in particular, poses significant challenges for bootstrap approximations to the distribution of $H_n(\psi)$, as needed for the inference of spatial mean parameters. Specially, the spatial FDB introduced in Ng et al. (2021) cannot capture this component in general, unless the underlying process is assumed to be Gaussian in which case this variance component $\sigma_2^2 = 0$ becomes zero. As a consequence, in order to improve bootstrap inference for spatial data, one must first correctly estimate all variance components in (2.2) in the resampling mechanism used. For use in conjunction with spatial bootstrap, we next consider a spatial subsampling for the purpose of such variance estimation, as described in the following section.

3. Spatial Subsampling in Frequency Domain

3.1 Spatial subsampling variance estimators

Based on the observed spatial data $\{Z(\mathbf{s}) : \mathbf{s} \in \mathcal{D}_n \cap \mathbb{Z}^2\}$ lying within the spatial sampling region $\mathcal{D}_n \equiv [1, n_1] \times [1, n_2]$, subsampling aims to create several "smaller scale copies" of the original spatial data by using data blocks of smaller size $b_n \equiv n_1^{(b)} n_2^{(b)}$ with $n_k^{(b)} < n_k,\ k =$

$1,2$ (cf. Lahiri, 2003b; Sherman and Carlstein, 1994; Sherman, 1996, 1998) compared to $n = n_1 n_2$, where the block size $n_k^{(b)}$ and the original sample size n_k in each direction satisfy the relation $n_k^{(b)} \to \infty$ and $n_k^{-1} n_k^{(b)} \to 0$ as $n \to \infty$. In particular, we can define data blocks by all integer translates of a region $\mathcal{D}_b \equiv [1, n_1^{(b)}] \times [1, n_2^{(b)}]$ that lie inside the original sampling region $\mathcal{D}_n \equiv [1, n_1] \times [1, n_2]$; that is, each data block is of the form $\mathbf{j} + \mathcal{D}_b$ for an integer $\mathbf{j} \equiv (j_1, j_2)$ with components $j_k = 0, \ldots, n_k - n_k^{(b)}$, $k = 1, 2$. In total, there are, say $L \equiv (n_1 - n_1^{(b)} + 1)(n_2 - n_2^{(b)} + 1)$, such data blocks and, for simplicity, we denote the ℓ-data block as $\mathcal{B}_\ell$ for $\ell = 1, \ldots, L$. We then define a subsample periodogram for the ℓ-th block as

$$\mathcal{I}_{sub}^{(\ell)}(\boldsymbol{\omega}) \equiv (2\pi)^{-2} b_n^{-1} \left| \sum_{\mathbf{s} \in \mathcal{B}_\ell \cap \mathbb{Z}^2} Z(\mathbf{s})\, e^{-\iota \mathbf{s}^\top \boldsymbol{\omega}} \right|^2, \;\; \boldsymbol{\omega} \in \Pi^2,\; \ell = 1, \ldots, L.$$

The corresponding subsample analog of the mean statistic $\widehat{M}_n(\psi)$ can then be defined as

$$\widehat{M}_{sub}^{(\ell)}(\psi) \equiv (2\pi)^2 b_n^{-1} \sum_{\mathbf{j} \in \mathcal{J}_b} \psi(\boldsymbol{\omega}_{\mathbf{j},b}) \mathcal{I}_{sub}^{(\ell)}(\boldsymbol{\omega}_{\mathbf{j},b}),$$

where $\boldsymbol{\omega}_{\mathbf{j},b}$ and $\mathcal{J}_b$ are defined similar to $\boldsymbol{\omega}_{\mathbf{j},n}$ and $\mathcal{J}_n$ earlier, but based on the subsample sizes b_n rather than the original data size n. These lead to a collection of subsample versions $H_{sub}^{(\ell)}(\psi)$ of the target spectral quantity $H_n(\psi) \equiv n^{1/2}\{\widehat{M}_n(\psi) - M(\psi)\}$ as

$$H_{sub}^{(\ell)}(\psi) \equiv b_n^{1/2}\{\widehat{M}_{sub}^{(\ell)}(\psi) - \widetilde{M}_n(\psi)\},\; \ell = 1, \ldots, L,$$

with the subsample mean $\widetilde{M}_n(\psi) \equiv L^{-1} \sum_{\ell=1}^{L} \widehat{M}_{sub}^{(\ell)}(\psi)$ as proxy for the parameter $M(\psi)$.

Recall that spatial variance estimation is especially important here because the variance σ^2 of spectral mean statistics from (2.2) can be quite complex or difficult to determine accurately, which is our motivation for consideration of subsampling. Consequently, we can define the subsampling variance estimator of σ^2 as

$$\widehat{\sigma}_n^2 = \widehat{\sigma}_n^2(\psi) \equiv \int_{\mathbb{R}} z^2 d\widehat{F}_{H_n(\psi)}(z) = L^{-1} \sum_{\ell=1}^{L} b_n \{\widehat{M}_{sub}^{(\ell)}(\psi) - \widetilde{M}_n(\psi)\}^2, \tag{3.3}$$

which corresponds to the sample variance of the subsample statistics $\{H^{(\ell)}_{sub}(\psi) \equiv b_n^{1/2}\{\widehat{M}^{(\ell)}_{sub}(\psi) - \widetilde{M}_n(\psi)\}_{\ell=1}^{L}$. Further, using subsampling, we also introduce an estimator for just the first variance component σ_1^2 in (2.2) as

$$\widehat{\sigma}^2_{1,n} \equiv b_n^{-1}(4\pi^2)^2 \sum_{\mathbf{j}\in\mathcal{J}_b} \psi(\boldsymbol{\omega}_{\mathbf{j},b})(\psi(\boldsymbol{\omega}_{\mathbf{j},b}) + \psi(\boldsymbol{\omega}_{-\mathbf{j},b}))\frac{1}{L}\sum_{\ell=1}^{L}(\mathcal{I}^{(\ell)}_{sub}(\boldsymbol{\omega}_{\mathbf{j},b}) - \widetilde{\mathcal{I}}_n(\boldsymbol{\omega}_{\mathbf{j},b}))^2, \tag{3.4}$$

where $\widetilde{\mathcal{I}}_n(\boldsymbol{\omega}_{\mathbf{j},b}) \equiv L^{-1}\sum_{\ell=1}^{L}\mathcal{I}^{(\ell)}_{sub}(\boldsymbol{\omega}_{\mathbf{j},b})$. Here in (3.4), we are isolating a component from the overall subsampling variance estimator $\widehat{\sigma}^2_n$ in (3.3) that arises due to marginal variance in subsample periodogram copies $\{\mathcal{I}^{(\ell)}_{sub}(\boldsymbol{\omega}_{\mathbf{j},b})\}_{\ell=1}^{L}$. This leads to a second subsampling estimator

$$\widehat{\sigma}^2_{2,n} \equiv \widehat{\sigma}^2_n - \widehat{\sigma}^2_{1,n} \tag{3.5}$$

to approximate the second or remaining component σ_2^2 in (2.2). Spatial subsampling then enables a valid estimation of both variance components σ_1^2 and σ_2^2 which contribute to the target distribution of $H_n(\psi)$ having a limit variance of $\sigma^2 \equiv \sigma_1^2 + \sigma_2^2$.

3.2 Consistency of spatial subsampling estimators

To establish the formal consistency properties for subsampling variance estimators with spectral mean statistics, we use the following mild assumptions. Assumptions 1-2 are standard for ensuring that the target quantity $H_n(\psi)$ in (2.2) has a limit law with finite variance σ^2.

Assumption 1. $\{Z(\mathbf{s}) : \mathbf{s} \in \mathbb{Z}^2\}$ is 4-th order stationary with summable covariances and 4-th order cumulants in the sense that $\sum_{\mathbf{s}\in\mathbb{Z}^2}(1 + \|\mathbf{s}\|)|\mathrm{Cov}(Z(\mathbf{0}), Z(\mathbf{s}))| < \infty$ and $\sum_{\mathbf{s}_1,\mathbf{s}_2,\mathbf{s}_3\in\mathbb{Z}^2}|\mathrm{cum}(Z(\mathbf{0}), Z(\mathbf{s}_1), z(\mathbf{s}_2), z(\mathbf{s}_3))| < \infty$, where $\|\cdot\|$ denotes the Euclidean norm.

Assumption 2. The normal limit exists in (2.2) for any ψ of bounded variation.

We require two additional Assumptions 3-4 below, which are related to Assumptions 1-2, but typically weaker (i.e., spatial processes fulfilling 1-2 typically then satisfy 3-4; cf. Remark 1). Assumptions 3-4 entail that dependence should decrease between certain statistics computed on distant observational regions, which is necessary for the validity of subsampling estimation (cf. Theorem 3.1) that relies on data blocks to provide spatial replication.

For two sequences $\mathbf{j}^{(n)} \equiv (j_1^{(n)}, j_2^{(n)}), \mathbf{k}^{(n)} \equiv (k_1^{(n)}, k_2^{(n)}) \in \mathbb{Z}^2$ of integer pairs, define $H_{\mathbf{j}^{(n)},n}(\psi)$ and $H_{\mathbf{k}^{(n)},n}(\psi)$ as versions of $H_n(\psi)$ when computed from translated spatial regions $\mathbf{j}^{(n)} + \mathcal{D}_n$ and $\mathbf{k}^{(n)} + \mathcal{D}_n$, instead of the region $\mathcal{D}_n \equiv [1, n_1] \times [1, n_2]$ used for $H_n(\psi)$ in (2.2).

Assumption 3. For any two $\mathbf{j}^{(n)}$ and $\mathbf{k}^{(n)}$ integer sequences where $\max_{i=1,2}(|j_i^{(n)} - k_i^{(n)}|/n_i) \to \infty$ as $n \equiv n_1 n_2 \to \infty$, the following quantities are asymptotically normal and independent:

$$\begin{pmatrix} H_{\mathbf{j}^{(n)},n}(\psi) \\ H_{\mathbf{k}^{(n)},n}(\psi) \end{pmatrix} \xrightarrow{D} \mathcal{N}\left(\begin{pmatrix} 0 \\ 0 \end{pmatrix}, \sigma^2 \begin{pmatrix} 1 & 0 \\ 0 & 1 \end{pmatrix} \right) \quad \text{as } n \to \infty.$$

For two integer sequences $\mathbf{j}^{(n)}, \mathbf{k}^{(n)} \in \mathbb{Z}^2$, we use one further assumption stated below that relates to the periodogram, say $\mathcal{I}_{\mathbf{j}^{(n)},n}(\boldsymbol{\omega})$ and $\mathcal{I}_{\mathbf{k}^{(n)},n}(\boldsymbol{\omega})$, when computed on translated sampling regions $\mathbf{j}^{(n)} + \mathcal{D}_n$ and $\mathbf{k}^{(n)} + \mathcal{D}_n$, respectively, for $\boldsymbol{\omega} \in \Pi^2 \equiv [-\pi, \pi]^2$.

Assumption 4. Let $\mathbf{m}_n \equiv (m_{n_1}, m_{n_2}) \in \mathbb{Z}^2$ with $0 \le |m_{n_i}| \le n_i - \lfloor n_i/2 \rfloor, i = 1, 2$ be an integer sequence such that the discrete Fourier frequencies $\boldsymbol{\omega}_{\mathbf{m}_n,n}$ converge to some limit $\boldsymbol{\omega} \equiv (\omega_1, \omega_2)$ with $0 < |\omega_i| < \pi$, $i = 1, 2$, as $n \equiv n_1 n_2 \to \infty$. For any two $\mathbf{j}^{(n)}$ and $\mathbf{k}^{(n)}$ integer sequences where $\max_{i=1,2}(|j_i^{(n)} - k_i^{(n)}|/n_i) \to \infty$ as $n \to \infty$, the periodogram ordinates are asymptotically exponential and independent:

$$\begin{pmatrix} \mathcal{I}_{\mathbf{j}^{(n)},n}(\boldsymbol{\omega}_{\mathbf{m}_n,n}) \\ \mathcal{I}_{\mathbf{k}^{(n)},n}(\boldsymbol{\omega}_{\mathbf{m}_n,n}) \end{pmatrix} \xrightarrow{D} f(\boldsymbol{\omega}) \begin{pmatrix} U_1 \\ U_2 \end{pmatrix} \quad \text{as } n \to \infty$$

where U_1, U_2 denote i.i.d standard exponential random variables.

For context, Assumption 3 intends a general, but mild, characterization of weak spatial dependence connected to Assumptions 1-2. This condition states that any copies $H_{\mathbf{j}^{(n)},n}(\psi)$

and $H_{\mathbf{k}^{(n)},n}(\psi)$ of the statistical quantity of interest $H_n(\psi)$, similarly defined on size $n \equiv n_1 n_2$ regions but of a diverging distance as $n \to \infty$, should be normal like $H_n(\psi)$ but also asymptotically independent; in particular, the spatial regions $\mathbf{j}^{(n)} + \mathcal{D}_n$ and $\mathbf{k}^{(n)} + \mathcal{D}_n$ for defining $H_{\mathbf{j}^{(n)},n}(\psi)$ and $H_{\mathbf{k}^{(n)},n}(\psi)$ have a distance

$$\text{dist}_n \equiv \min\left\{\|\mathbf{s} - \mathbf{t}\| : \mathbf{s} \in \mathbf{j}^{(n)} + \mathcal{D}_n,\, \mathbf{t} \in \mathbf{k}^{(n)} + \mathcal{D}_n\right\} \geq \max_{i=1,2}\left(|j_i^{(n)} - k_i^{(n)}| - n_i\right) \to \infty \quad (3.6)$$

that grows as $n \to \infty$, because ith component of the difference $\mathbf{j}^{(n)} - \mathbf{k}^{(n)}$ diverges faster than the sample size n_i in some direction, $i = 1, 2$, in Assumption 3. For such regions, a natural characterization of weak dependence is that quantities $H_{\mathbf{j}^{(n)},n}(\psi)$ and $H_{\mathbf{k}^{(n)},n}(\psi)$ should be independent as $n \to \infty$. Assumption 4 is analogous to Assumption 3 in spirit, but weaker, saying that spatial periodograms computed from distant regions should be asymptotically independent and exponentially distributed up to scaling by the spectral density f. Assumptions 1-4 can hold for many spatial processes, and we provide some examples next.

As perhaps the most straightforward example, an m-dependent stationary spatial process with $E[Z(\mathbf{s})]^4 < \infty$ satisfies Assumptions 1-4 (i.e., where two observations $Z(\mathbf{s})$ and $Z(\mathbf{t})$ are independent if $\|\mathbf{s} - \mathbf{t}\| > m$ for some distance $m > 0$); in particular, the independence of statistics in Assumption 3 holds by (3.6) in this case. Examples of such processes can include Gaussian nearest-neighbor models (cf. Datta et al., 2016). Another standard spatial process where Assumptions 1-4 hold is given by linear spatial processes $Z(\mathbf{s}) = \mu + \sum_{\mathbf{k}\in\mathbb{Z}^2} a_{\mathbf{k}}\varepsilon(\mathbf{s} - \mathbf{k})$ defined by i.i.d. (perhaps non-Gaussian) innovations $\{\varepsilon(\mathbf{k}) : \mathbf{k} \in \mathbb{Z}^2\}$ with $E[\varepsilon(\mathbf{k})] = 0$ and $E[\varepsilon(\mathbf{k})]^4 < \infty$ and real-valued coefficients that are summable $\sum_{\mathbf{k}\in\mathbb{Z}^2} \|\mathbf{k}\||a_{\mathbf{k}}| < \infty$. These processes have a long history of consideration in statistics and econometrics (cf. Tjøstheim, 1978; Anselin, 1988; Guyon, 1995), and Assumptions 1-4 can be verified by approximating such processes with tail-truncated versions $\mu + \sum_{\|\mathbf{k}\|<m/2} a_{\mathbf{k}}\varepsilon(\mathbf{s} - \mathbf{k})$ (i.e., for suitably large m)

that are m-dependent. A further general class of spatial processes that fulfill Assumptions 1-4 include so called α-mixing processes, which are commonly considered in resampling developments (cf. Lahiri, 2003b); see Remark 1 for technical details. Non-Gaussian examples of such processes can include spatial Markov random fields, having conditionally specified distributions that may be beta, binary, Poisson, or more general exponential families (cg. Besag, 1974; Caragea and Kaiser, 2009; Hardouin and Yao, 2008; Kaiser et al., 2002). In particular, when such conditional model specifications satisfy Dobrushin's uniqueness condition (cf. Guyon, 1995), then the Markov random field is α-mixing (actually, stronger ϕ-mixing).

We can next state a formal result on the consistency of subsampling variance estimators.

Theorem 3.1. Suppose Assumptions 1-4 hold and the subsample size $b_n \equiv n_1^{(b)} n_2^{(b)}$ satisfies $1/n_k^{(b)} + n_k^{-1} n_k^{(b)} \to 0$ for $k = 1, 2$ as $n \equiv n_1 n_2 \to \infty$. Then, the spatial subsampling estimators of variance components are consistent:

$$\widehat{\sigma}^2_{1,n} \xrightarrow{P} \sigma_1^2, \quad \widehat{\sigma}^2_{2,n} \xrightarrow{P} \sigma_2^2, \quad \text{and} \quad \widehat{\sigma}^2_n \xrightarrow{P} \sigma^2 \equiv \sigma_1^2 + \sigma_2^2 \quad \text{as } n \to \infty.$$

The theorem above provides a device to modify and improve spatial bootstraps for approximating spectral mean statistics, particularly when such bootstraps can fail to appropriately reflect the spreads of such statistics. This then leads to the spatial hybrid bootstrap procedure proposed in the next section.

Remark 1. For completeness, we state α-mixing conditions for verifying Assumptions 1-4. For a subset $T \subset \mathbb{Z}^2$ of spatial locations, let $|T|$ denote the cardinality and let $\mathcal{F}_Z(T) \equiv \sigma\langle Z(\mathbf{s}) : \mathbf{s} \in T\rangle$ denote the σ-algebra generated by observations $Z(\mathbf{s})$, $\mathbf{s} \in T$. Define a dependence measure $\tilde{\alpha}(T_1, T_2) \equiv \sup\{|P(A_1 \cap A_2) - P(A_1)P(A_2)| : A_1 \in \mathcal{F}_Z(T_1), A_2 \in \mathcal{F}_Z(T_2)\}$ and distance $d(T_1, T_2) \equiv \min\{\|\mathbf{s}_1 - \mathbf{s}_2\| : \mathbf{s}_1 \in T, \mathbf{s}_2 \in T_2\}$ between two subsets

$T_1, T_2 \subset \mathbb{Z}^2$. Denote the mixing coefficient of the spatial process $\alpha(a,b) \equiv \sup\{\tilde{\alpha}(T_1,T_2) : d(T_1,T_2) \geq a, \max\{|T_1|,|T_2|\} \leq b\}$ as a function of the distance $a > 0$ and size $b > 0$ of two sets of spatial locations. Assuming $\alpha(a,b) \leq \alpha_1(a)g(b)$ holds for a non-increasing function $\alpha_1(\cdot)$ and a non-decreasing function $g(\cdot)$ as in Lahiri (2003a), results in the latter (Prop 4.2, Theorem 4.2) can be used to show that Assumption 1 holds if $\sup_{\mathbf{s}\in\mathbb{Z}^2} E[Z(\mathbf{s})]^{4+\delta} < \infty$ along with $\alpha_1(a) = O(a^{-\tau})$ as $a \to \infty$ for some $\delta > 0$ and $\tau > 6(4+\delta)/\delta$, while Assumption 2 also holds if $g(b) = o(b^{(\tau-2)/8})$ as $b \to \infty$ and the directional sizes n_1, n_2 of a sampling region are proportional (or $\max\{n_1,n_2\}/\min\{n_1,n_2\}$ is bounded). Such conditions further imply Assumptions 3-4, as the dependence between the two sets/statistics in 3-4 is measured by $\alpha(\mathrm{dist}_n, n) = O(n_1^{-\tau} n^{(\tau-2)/8}) \to 0$ as $n = n_1 n_2 \to \infty$ for dist_n in (3.6).

4. Spatial Hybrid Frequency Domain Bootstrap (HFDB)

We may now describe our main resampling approach for approximating the distribution of spatial spectral mean statistics. Recall that, as explained in the Introduction, Ng et al. (2021) proposed a bootstrap for spatial data, which is generally invalid for inference about spectral averages and requires modification for capturing the complicated variance of spectral averages. For reference, we shall term their bootstrap method as technically being a Frequency Domain Wild Bootstrap (FDWB). Recently, for the case of time series data, Meyer et al. (2020) and Yu et al. (2023) described a hybrid periodogram bootstrap (HPB) as the most advanced resampling scheme for spectral mean inference with time series in terms of broad validity and performance. Our hybrid resampling approach for spatial data, termed the Hybrid Frequency Domain Bootstrap (HFDB), intends types of extensions of both FDWB and HPB methods. That is, the spatial HFDB aims to combine spatial bootstrap (i.e., FDWB) with spatial subsampling (Sec. 3.1) in order to correct scaling issues in bootstrap for spatial data. This also produces a spatial analog version of HPB from time series.

For setting distributional approximations for spatial spectral mean statistics, both HFDB and FDWB approaches start with a common step of mimicking the distribution of spectral statistics by a scheme of independently resampling or re-creating periodogram values based on an estimator $\widehat{f}_n$ of the spectral density f. To this end, let $\widehat{f}_n$ represent a consistent estimator of the spectral density f across spatial discrete Fourier frequencies, i.e.

$$\max_{\mathbf{j}\in\mathcal{J}_n}|\widehat{f}_n(\boldsymbol{\omega}_{\mathbf{j},n}) - f(\boldsymbol{\omega}_{\mathbf{j},n})| = o_P(1) \text{ as } n \to \infty. \tag{4.7}$$

Note that all FDB approaches involve spectral density estimation, which is true for time series (cf. Dahlhaus and Janas, 1996; Jentsch and Kreiss, 2010; Kreiss and Paparoditis, 2003; Meyer et al., 2020) and for FDWB with spatial data (Ng et al., 2021). We then define an initial bootstrap re-creation of the target spectral mean quantity $H_n(\psi)$ from (2.2) as

$$Q^*_{FDWB,n}(\psi) \equiv n^{1/2}\{(2\pi)^2 n^{-1} \sum_{\mathbf{j}\in\mathcal{J}_n} \psi(\boldsymbol{\omega}_{\mathbf{j},n})\widehat{f}_n(\boldsymbol{\omega}_{\mathbf{j},n})(U^*_{\mathbf{j}} - 1)\} \tag{4.8}$$

by drawing $U^*_{\mathbf{j}}$ as i.i.d exponential random variables for indices $\mathbf{j} \equiv (j_1, j_2) \in \mathcal{J}_n$ involving $j_1 > 0$ or involving $j_1 = 0$ with $j_2 > 0$ and then setting $U^*_{-\mathbf{j}} \equiv U^*_{\mathbf{j}}$ for the remaining indices $\mathbf{j} \in \mathcal{J}_n$ (i.e., where $j_1 < 0$ or where $j_1 = 0$ with $j_2 < 0$). Note that the bootstrap approximation in (4.8) corresponds to the FDWB of Ng et al. (2021) for spatial data and also represents a basic step in any FDB with time series (cf. Meyer et al., 2020). This bootstrap form aims to produce bootstrap versions $\{U^*_{\mathbf{j}}\widehat{f}_n(\boldsymbol{\omega}_{\mathbf{j},n})\}$ of the periodogram ordinates $\{\mathcal{I}_n(\boldsymbol{\omega}_{\mathbf{j},n})\}$ (i.e., indexed over $\mathbf{j} \in \mathcal{J}_n$), by treating the latter as approximately independent exponential variables with respective means $\{f(\boldsymbol{\omega}_{\mathbf{j},n})\}$. However, the problem in this bootstrap re-creation is that dependence among periodogram ordinates $\mathcal{I}_n(\boldsymbol{\omega}_{\mathbf{j},n})$, $\mathbf{j} \in \mathcal{J}_n$, is generally not completely ignorable so the bootstrap quantity $Q^*_{FDWB,n}(\psi)$ cannot correctly capture the true variance $\sigma^2 \equiv \sigma_1^2 + \sigma_2^2$ of $H_n(\psi)$ in (2.2). Essentially, by independently resampling or re-constructing spatial periodogram values by $\{U^*_{\mathbf{j}} \widehat{f}_n(\boldsymbol{\omega}_{\mathbf{j},n})\}$, the resulting FDWB in (4.8) then estimates the second variance component σ_2^2 to be zero, where the latter may not hold in general for the underlying spatial process (i.e., unless the process is assumed to be Gaussian).

To overcome the above shortcoming in FDWB, a scaling adjustment with spatial subsampling can be made to define a hybrid FDB (HFDB) rendition of $H_n(\psi)$ as

$$H^*_{HFDB,n}(\psi) \equiv [\mathrm{Var}_*\{Q^*_{FDWB,n}(\psi)\} + \widehat{\sigma}^2_{2,n}]^{1/2} \frac{Q^*_{FDWB,n}(\psi)}{[\mathrm{Var}_*\{Q^*_{FDWB,n}(\psi)\}]^{1/2}}, \tag{4.9}$$

where we first re-scale (4.8) to have unit variance at the bootstrap level using the bootstrap variance of $\{Q^*_{FDWB,n}(\psi)\}$ given by

$$\mathrm{Var}_*\{Q^*_{FDWB,n}(\psi)\} = n^{-1}(4\pi^2)^2 \sum_{\mathbf{j}\in\mathcal{J}_n} \psi(\boldsymbol{\omega}_{\mathbf{j},n})(\psi(\boldsymbol{\omega}_{\mathbf{j},n}) + \psi(\boldsymbol{\omega}_{-\mathbf{j},n}))\widehat{f}^2_n(\boldsymbol{\omega}_{\mathbf{j},n})$$

and then introduce a correction $\mathrm{Var}_*\{Q^*_{FDWB,n}(\psi)\} + \widehat{\sigma}^2_{2,n}$ to estimate the correct target variance $\sigma^2 \equiv \sigma_1^2 + \sigma_2^2$; this scaling correction $\mathrm{Var}_*\{Q^*_{FDWB,n}(\psi)\} + \widehat{\sigma}^2_{2,n}$ combines the original bootstrap variance $\mathrm{Var}_*\{Q^*_{FDWB,n}(\psi)\}$ as an approximation of the first variance component σ_1^2, with a subsampling variance estimator $\widehat{\sigma}^2_{2,n} = \widehat{\sigma}^2_n - \widehat{\sigma}^2_{1,n}$ from (3.5) that approximates the second component σ_2^2. In this manner, the hybrid bootstrap approximation $H^*_{HFDB,n}(\psi)$ in (4.9) can capture the correct spread in addition to the shape of the target sampling distribution of $H_n(\psi)$ for spectral inference. In the HFDB method, note that spatial subsampling plays a role in specifically estimating the variance component σ_2^2 that would otherwise be missed by FDWB, while the bootstrap variance $\mathrm{Var}_*\{Q^*_{FDWB,n}(\psi)\}$ from FDWB continues to estimate the first component σ_1^2 as implicit in (4.8). The next result provides a broad theoretical justification for the HFDB method.

Theorem 4.1. Suppose assumptions of Theorem 3.1 along with (4.7). Then, for the HFDB version $H^*_{HFDB,n}(\psi)$ of $H_n(\psi)$,

(a) HFDB spread is consistent for the limit variance $\sigma^2 \equiv \sigma_1^2 + \sigma_2^2$ of $H_n(\psi)$:

$$\mathrm{Var}_*\{H^*_{HFDB,n}(\psi)\} = \mathrm{Var}_*\{Q^*_{FDWB,n}(\psi)\} + \widehat{\sigma}^2_{2,n} \xrightarrow{P} \sigma^2 \text{ as } n \to \infty.$$

(b) the HFDB approximation is consistent for the target distribution of $H_n(\psi)$:

$$\sup_{x\in\mathbb{R}} \left| P_*(H^*_{HFDB,n}(\psi) \le x) - P(H_n(\psi) \le x) \right| \xrightarrow{P} 0 \quad \text{as } n \to \infty,$$

where $P_*(\cdot)$ denotes bootstrap probability induced by resampling.

Because the HFDB approach combines bootstrap with spatial subsampling, Theorem 4.1 shows that HFDB achieves consistency for distributional approximations of spectral means statistics under less stringent moment assumptions than previous spatial bootstraps (cf. Ng et al., 2021). Furthermore, the methodology presented above for spatial HFDB can then be applied to both Gaussian and non-Gaussian processes, while the original FDWB can only be applied to Gaussian spatial data. Numerical results in Section 5 further demonstrate that the HFDB can perform well, including cases where FDWB is inadequate.

Remark 2. As a further observation, we can decompose the target quantity $H_n(\psi)$ as

$$H_n(\psi) \equiv n^{1/2}\{\widehat{M}_n(\psi) - M(\psi)\} = n^{1/2}\{\widehat{M}_n(\psi) - E(\widehat{M}_n(\psi))\} + n^{1/2}\{E(\widehat{M}_n(\psi)) - M(\psi)\},$$

where the first part in the decomposition is a stochastic quantity with mean zero while the second part can be treated as a non-stochastic bias. While the above bias decreases to zero with increasing spatial sample size n, this bias term can potentially impact approximations in small sample sizes. Therefore, in small samples, it is also possible to consider spatial subsampling for estimating this bias part as $\widehat{\text{Bias}}_{\text{sub}} \equiv L^{-1}\sum_{\ell=1}^{L} b_n^{1/2}(\widehat{M}_{\text{sub}}^{(\ell)}(\psi) - \widehat{M}_n(\psi))$. In which case, we can use $H^*_{HFDB,n} + \widehat{\text{Bias}}_{\text{sub}}$ as a bootstrap approximation to $H_n(\psi)$, which uses subsampling to adjust bootstrap approximations $Q^*_{FDWB,n}(\psi)$ from (4.8) for both variance as in (4.9) as well as for bias. We numerically examine such bias adjustments in Section 5.

4.1 Implementation of HFDB in practice

Implementing HFDB requires selecting both a block/subsample size and a kernel-based spectral density estimator in a principled manner. For block sizes, one may consider blocks $\mathcal{D}_b = [1, n_1^{(b)}] \times [1, n_2^{(b)}]$ defined by scaling $n_k^{(b)} \approx Cn^{1/4} = C(n_1 n_2)^{1/4}$, $k = 1, 2$, for some $C > 0$ (often with $C = 1, 1.5$, or 2). Such choice corresponds to an optimal size order for subsampling variance estimation (Nordman and Lahiri, 2004). This rule of thumb is fast to implement and is illustrated in numerical studies of Section 5. Other related, but more computationally demanding, approaches for block selection include the minimum volatility principle of Politis et al. (1999) and the non-parametric plug-in (NPPI) method from Lahiri et al. (2007). The first approach involves computing bootstrap intervals over a range of block sizes and choosing a block around which the intervals do not change substantially according to some criterion (e.g., length). NPPI estimates optimal block scalings $n_1^{(b)} = n_2^{(b)}$ for variance estimation with a similar formula $\hat{C}n^{1/4}$ as above, through the constant $\hat{C}$ is estimated through additional steps requiring Jackknife-After-Bootstrap.

For estimating the spectral density $f(\omega)$, $\boldsymbol{\omega} \in \Pi^2$, a suitable bivariate kernel function (e.g., Gaussian, Epanechnikov) may be used together with appropriate bandwidths (δ_1, δ_2), where Ng et al. (2021) suggest choosing a bandwidth of the form $\delta_1 = \delta_2$ with $\delta_k \in [0.05, 0.15]$ for small to moderate sample sizes. We standardly use $\delta_1 = \delta_2 = 0.05, 0.1$, or 0.15 with a standard bivariate Gaussian kernel in Section 5, which performed well with HFDB and also corresponds to the scheme for spectral density estimation with FDWB (Ng et al., 2021).

Once block sizes and kernel bandwidths are specified, HFDB can be used to generate bootstrap replicates for calibrating hypothesis tests and confidence intervals in the frequency domain. We recommend using at least 500 bootstrap replications, as done in Section 5.

5. Numerical Studies

Here we examine the finite sample performance of the HFDB approximation of spatial spectral statistics over several inference problems, with comparisons to the FDWB approximation of Ng et al. (2021) (cf. Section 4). Theory from Sections 3-4 suggests that HFDB should apply regardless of whether the underlying process is Gaussian or not (i.e., even when the variance component σ_2^2 from (2.2) is not zero as can occur in practice for non-Gaussian data). In cases where σ_2^2 is exactly zero (i.e., Gaussian processes), HFDB is anticipated to perform similarly to FDWB. In the following, we present numerical results for scenarios including Gaussian processes as well as a non-Gaussian processes. For each spatial sample size and process type in the following, we performed 1000 simulation runs to evaluate coverages and 500 replications per simulated dataset to approximate bootstrap distributions. For both FDWB/HFDB, spectral density estimation uses a Gaussian kernel with bandwidth $(\delta_1, \delta_2) = (0.05, 0.05)$, as in Section 4.1 and Ng et al. (2021), unless otherwise stated. Further simulation results, including additional coverage and bandwidth studies, appear in Supplementary Materials. The HFDB method shall also implement a bias adjustment (Remark 2) throughout; as shown in Section 5.1, the effect of this adjustment is modest for coverage, but can offer improvements.

5.1 Confidence intervals for spatial covariance

We initially consider interval estimation of spatial covariance parameters $\gamma(\mathbf{h}) \equiv \mathrm{Cov}(Z(\mathbf{0}), Z(\mathbf{h}))$, $\mathbf{h} \in \mathbb{Z}^2$, as corresponding to a spectral mean $M(\psi)$ in (2.1) with $\psi(\boldsymbol{\omega}) = \cos(\mathbf{h}^\top \boldsymbol{\omega})$. A main interest is comparing the performances of HFDB and FDWB approximations for calibrating intervals, though we also consider alternative interval constructions through standard normal approximations of sample covariances combined with variance estimation steps. We focus on nominal 95% confidence intervals, where bootstrap intervals have equi-tailed form $[\widehat{M}_n(\psi) - \widehat{q}_{0.975} n^{-1/2}, \widehat{M}_n(\psi) - \widehat{q}_{0.025} n^{-1/2}]$ based on quantiles $\widehat{q}_{0.025}$ and $\widehat{q}_{0.975}$ of bootstrap distributions approximated by 500 bootstrap draws for any data set. We consider rectangular spatial datasets of sizes 30×30 $(n = 900), 50 \times 50$ $(n = 2500)$, and 70×70 $(n = 4900)$.

As a first study, we consider a real-valued mean-zero spatial Gaussian process with a covariance function is given by $\gamma(\mathbf{h}) = \theta^2 \exp\left(-(\|\mathbf{h}\|/\phi)^2\right)$, where θ^2 is the partial sill parameter and ϕ is the range parameter. For simulation, we set $\theta^2 = 1$ and $\phi = 2$, with no nugget effect. This allows evaluation of the interval methods for Gaussian data, where the latter presents less higher-order dependence to complicate spectral inference. Figure 1 presents the coverage accuracy of 95% two-tailed confidence intervals for the covariance parameter $\gamma(\mathbf{h})$ over multiple lags $\mathbf{h} = (1,0)^\top, (0,1)^\top, (1,1)^\top$; note that HFDB coverages are plotted over various (square) block sizes b_n while FDWB coverages do not depend on blocks and so plot as straight lines. From Figure 1, we observe that, as the overall spatial sample size n increases, both HFDB/FDWB methods show coverage accuracies that behave similarly and approach the nominal value for all lags. This feature suggests that both HFDB and FDWB are valid for the Gaussian process (i.e., with $\sigma_2^2 = 0$), as expected, where such similarity is anticipated to occur in this case because HFDB involves a scaling correction to

FDWB that is intended to be most impactful when σ_2^2 in (2.2) is non-zero. Vertical lines in Figure 1 also indicate that HFDB coverages by the rule for block selection from Section 4.1 (with $C = 1$ for illustration) appear adequate.

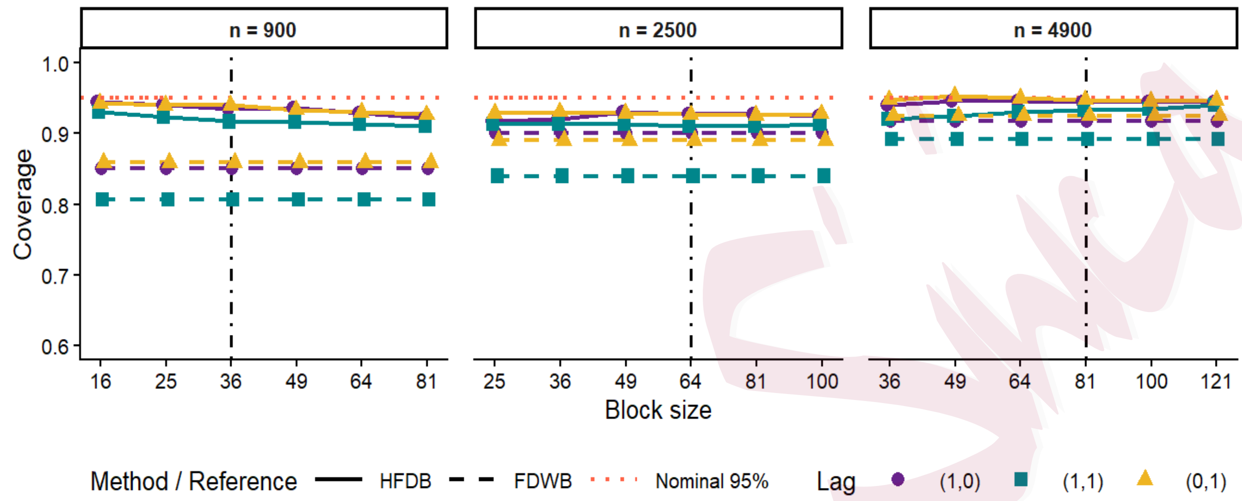

Figure 1: For covariance parameters $\gamma(\mathbf{h})$ at different lags $\mathbf{h}$, coverages of 95% HFDB/FDWB intervals over various sample sizes n; HFDB coverages are a function of (square) block size b_n, where the vertical line indicates a rule of thumb block choice.

As a non-Gaussian case, we generate a spatial field defined by $Z(\mathbf{s}) \equiv \sum_{u=0}^{2}\sum_{v=0}^{2} a_{u,v}\varepsilon(s_1 - u, s_2 - v)$, for $\mathbf{s} \equiv (s_1, s_2) \in \mathbb{Z}^2$, with i.i.d. innovations $\{\varepsilon(\mathbf{s}) \equiv X(\mathbf{s}) - E[X(\mathbf{s})] : \mathbf{s} \in \mathbb{Z}^2\}$ using $X(\mathbf{s}) \sim \text{Gamma}(1/5, \sqrt{5})$ and filter coefficients $a_{u,v} = [A]_{u+1,v+1}/\|A\|$, $u, v \in \{0, 1, 2\}$ defined by entries $[A]_{u+1,v+1}$ of the matrix

$$A = \begin{pmatrix} 1 & 0.3 & 0.1 \\ 0.5 & 0.2 & 0.1 \\ 0.25 & 0.1 & 0.05 \end{pmatrix}$$

and scaled by the Euclidean norm $\|A\|$ so that $\sum_{u,v} a_{u,v}^2 = 1$. Linear spatial processes are common in spatial statistics, and this construction produces a strongly non-Gaussian field (e.g., skewness and excess kurtosis) with unit variance and a non-zero fourth-order cumulant structure. The latter feature implies that a variance component $\sigma_2^2 > 0$ impacts the distribution of spectral statistics, which the HFDB aims to accommodate. In conjunction with this process, we again consider interval estimation of covariance parameters $\gamma(\mathbf{h})$ at several lags $\mathbf{h} = (1,0)^\top, (0,1)^\top, (1,1)^\top$. Here the lag type has a pronounced influence on the distribution of covariance estimators targeted by bootstrap approximation, where horizontal or vertical lags $\mathbf{h} \in \{(1,0)^\top, (0,1)^\top\}$ entail more dependence than a diagonal lag $\mathbf{h} = (1,1)^\top$, leading to larger variance components (e.g., σ_2^2) and more difficulties in estimation.

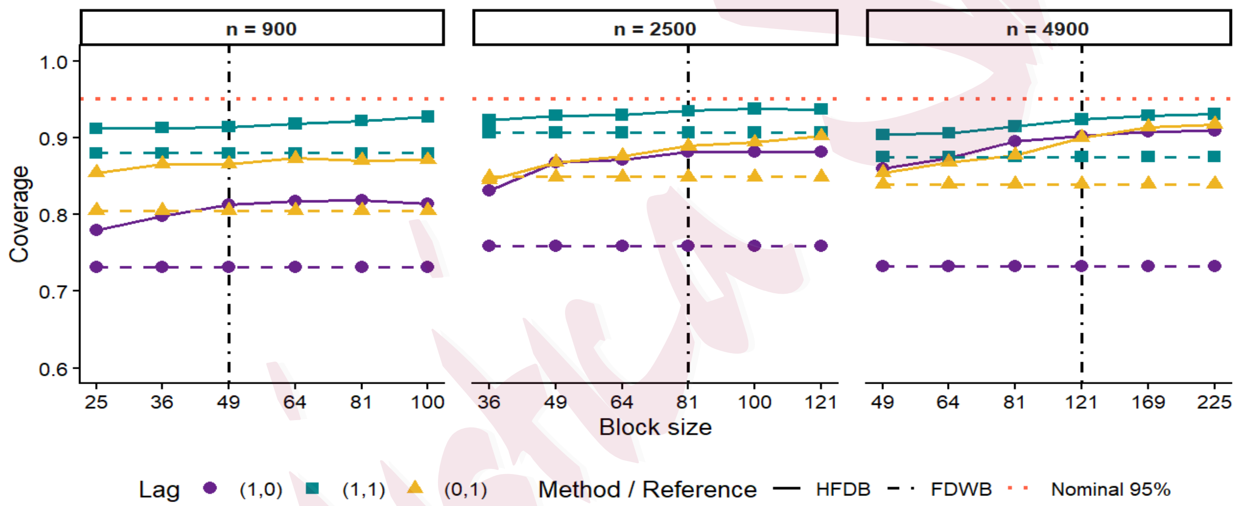

Figure 2: For covariance parameters $\gamma(\mathbf{h})$ at different lags $\mathbf{h}$, coverages of 95% HFDB/FDWB intervals over various sample sizes n; HFDB coverages are a function of (square) block size b_n, where the vertical line indicates a rule of thumb block choice.

Figure 2 displays the resulting coverages of HFDB/FDWB intervals, where HFDB coverages are again a function of block size b_n. For all covariance parameter lags, the HFDB method consistently outperforms the FDWB in coverage across all sample sizes. In contrast, FDWB exhibits systematic undercoverage due to underestimation of variance components

σ_2^2, which is most apparent with the lag $\mathbf{h} = (1, 0)^\top$ which induces the most dependence in estimation here (largest σ_2^2). In contrast, with $\mathbf{h} = (1, 1)^\top$, the contribution of σ_2^2 is smaller, whereby underestimation of variance by FDWB is less severe and coverage appears closer to HFDB. The coverage performance of HFDB is relatively stable across block sizes, and vertical lines in Figure 2 again indicate that coverages by the block rule described in Section 4.1 (with $C = 1.25$ for illustration) seem reasonable.

Considering this same non-Gaussian process, we may also compare HFDB intervals to alternative (i.e., non-bootstrap) intervals based on standard normal calibrations. In particular, we examine 95% intervals $\widehat{M}_n(\psi) \pm z_{0.975}\widehat{\sigma}_n n^{-1/2}$ based on a normal quantile $z_{0.975} = 1.96$ and a subsampling variance estimator $\widehat{\sigma}_n$ from (3.3) for the sample covariance quantity $\widehat{M}_n(\psi)$.

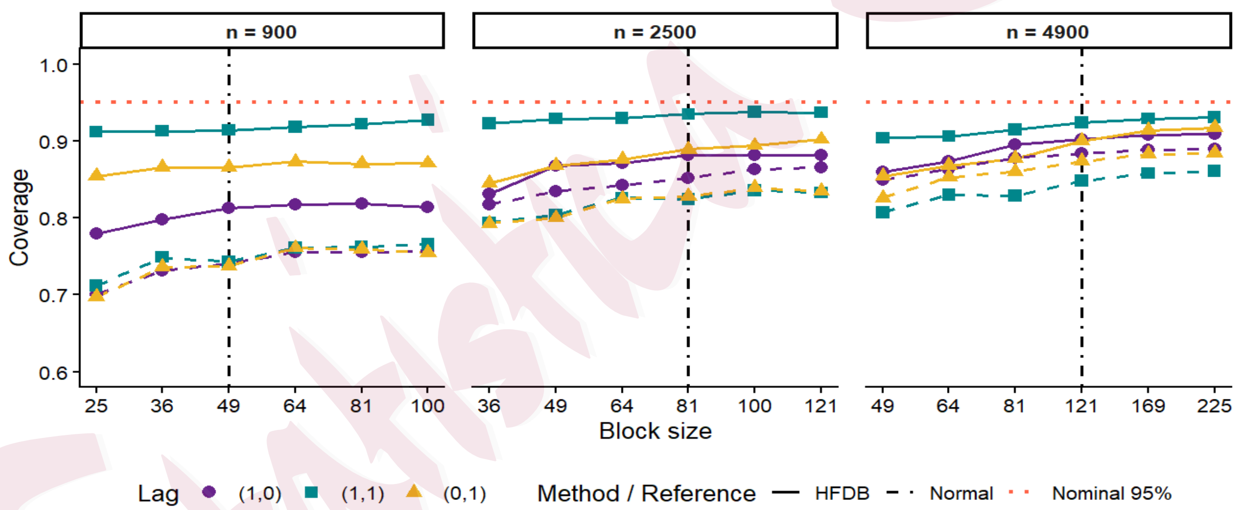

Figure 3: For covariance parameters $\gamma(\mathbf{h})$ at different lags $\mathbf{h}$, coverages of 95% HFDB/normal intervals over various sample sizes n; coverages of both intervals are a function of (square) block size b_n, where the vertical line indicates a rule of thumb block choice.

Figure 3 provides coverage comparisons between HFDB and normal-theory intervals, where this figure serves as a direct analog of Figure 2 after replacing FDWB intervals in the latter with normal intervals. In Figure 3, the coverages of both HFDB and normal intervals depend on block size b_n for variance estimation, though the techniques differ between these methods. For all covariance parameter lags, HFDB consistently outperforms normal intervals across block and sample sizes; the same is not necessarily true in comparing FDWB to normal intervals across Figures 2-3. Additional simulation results in Supplementary Materials also show that normal intervals also undercover for the previous Gaussian process as well.

As stated at the outset of Section 5, we have focused on using a bias adjusted version of HFDB (cf. Remark 2) for consistence. The effect of this adjustment is often modest and decreasing with increasing sample sizes n, but can be useful. As illustration with the non-Gaussian process, Table 1 provides a coverage comparison of HFDB intervals for a covariance $\gamma(\mathbf{h})$, $\mathbf{h} = (1, 0)^\top$, both with and without such bias adjustment. The adjustment provides modest improvements, uniformly across blocks, with less differences as sample size increases.

$n = 900$			$n = 2500$			$n = 4900$		
Block	W	W/O	Block	W	W/O	Block	W	W/O
5×5	78.0	76.2	6×6	83.1	82.5	7×7	86.1	84.9
6×6	79.8	76.7	7×7	86.8	84.3	8×8	87.4	86.0
$7 \times 7^*$	81.3	78.7	8×8	87.1	85.3	9×9	89.5	87.2
8×8	81.7	78.9	$9 \times 9^*$	88.2	85.8	$11 \times 11^*$	90.2	88.3
9×9	81.8	79.5	10×10	88.2	85.9	13×13	90.8	89.0
10×10	81.4	79.6	11×11	88.1	86.6	15×15	90.9	89.1

Table 1: For $\gamma(\mathbf{h})$, $\mathbf{h} = (1, 0)^\top$, coverage (%) of 95% HFDB intervals with (W) and without (W/O) bias adjustment over block and sample sizes; $*$ denotes a rule of thumb block choice.

5.2 Variogram model fitting for non-Gaussian processes

As another illustration, we examine the coverage performance of frequency-domain bootstrap methods for estimating a variogram model parameter. In particular, we compare FDWB with HFDB for the same non-Gaussian process from Section 5.1. We consider a working semi-variogram model of the form $\nu(\mathbf{h};\theta) \equiv \theta g_0(\mathbf{h})$ with $g_0(\mathbf{h}) \equiv 1 - \exp(-\|\mathbf{h}\|/\phi_0)$ for $\mathbf{h} \in \mathbb{Z}^2$, where $\phi_0 = 2.5$ and only the sill parameter $\theta > 0$ is estimated. Given a set of lags $\{\mathbf{h}_1, \ldots, \mathbf{h}_3\} \equiv \{(1,0),(1,1),(0,1)\}$, the parameter θ can be formulated through the least squares criterion defined in 2.2.

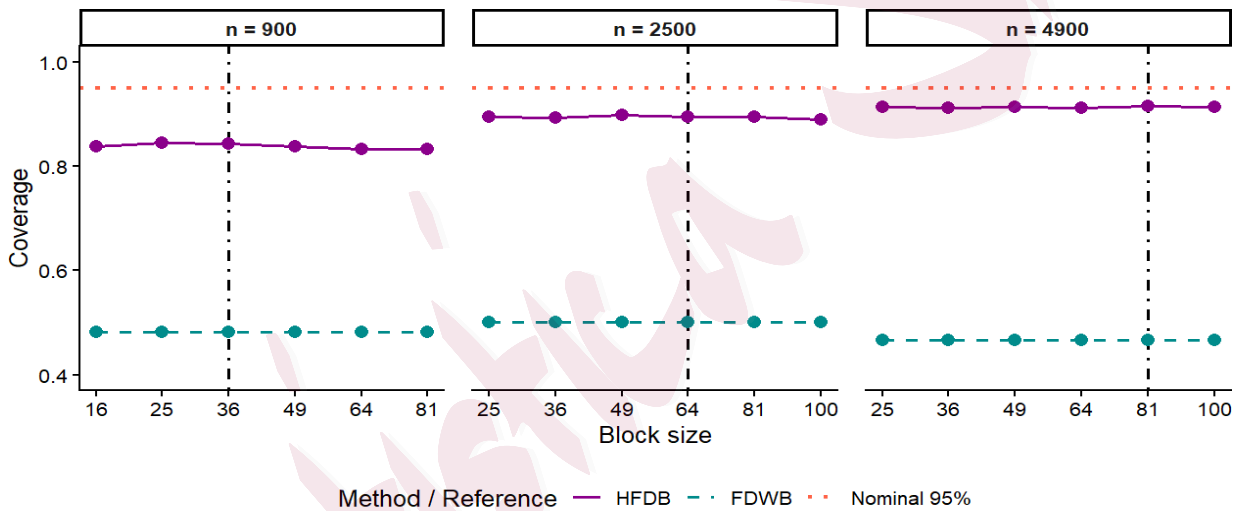

Figure 4: Coverages of 95% HFDB/FDWB intervals for the semi-variogram parameter with different sample sizes n; HFDB coverages are a function of (square) block size b_n, where the vertical line indicates a rule of thumb block choice.

For different sampling region sizes $n = 900, 2500, 4900$, Figure 4 shows the coverage rates of nominal 95% confidence intervals for the semi-variogram parameter θ based on FDWB and HFDB methods, with the latter coverages as a function of block size b_n. Here the

FDWB performs poorly due to an underestimation of variance, leading to a substantial undercoverage. In contrast, HFDB significantly improves coverage which approaches the nominal level as the sample size increases, exhibiting consistent performance across block sizes. The vertical line in Figure 4 also suggests good coverage by the block rule of thumb ($C = 1$ for illustration) from Section 4.1. For bootstrap inference, this numerical study further demonstrates the importance of accounting for higher-order dependence that can appear in the variance of frequency domain statistics with non-Gaussian spatial processes, where HFDB leads to more reliable inference.

5.3 Calibration of Spatial Isotropy Tests

Here we examine the performance of bootstrap methods when applied to tests of spatial isotropy (i.e., the covariance function of the stationary spatial process is rotationally invariant). To construct a test, we follow the setup of Guan et al. (2004), which has also been adopted in Ng et al. (2021). In particular, we consider testing the following hypothesis:

$$H_0 : 2\kappa(\mathbf{h}_i) = 2\kappa(\mathbf{h}_j), \text{ for all } \mathbf{h}_i, \mathbf{h}_j \in \Lambda, \ \mathbf{h}_i \neq \mathbf{h}_j, \text{ and } ||\mathbf{h}_i|| = ||\mathbf{h}_j||,$$

where $\Lambda \equiv \{\mathbf{h}_1, \mathbf{h}_2, \ldots, \mathbf{h}_m\}$ is a prespecified set of sites and $2\kappa(\mathbf{h}) \equiv E(Z(\mathbf{0}) - Z(\mathbf{h}))^2$ is the variogram at lag $\mathbf{h}$. Letting $G \equiv (2\kappa(\mathbf{h}_1), \ldots, 2\kappa(\mathbf{h}_m))$ denote the vector of variograms in Λ, Guan et al. (2004) proposed a test of spatial isotropy by assessing whether $AG = 0$ holds for a given full row rank matrix A of linear contrasts. The same test can also be written in terms of a spectral mean assessment of whether $M(\psi) = 0$ holds for various spectral mean functionals. For illustration, if we consider lags $\Lambda = \{\mathbf{h}_1, \mathbf{h}_2\}$ for $\mathbf{h}_1 \equiv (1, 0)$ and $\mathbf{h}_2 \equiv (0, 1)$ along $A = [-1 \quad 1]$, then the test of isotropy involves assessing whether spectral mean statistic $\widehat{M}_n(\psi)$ based on $\psi(\boldsymbol{\omega}) \equiv \{2\cos(\mathbf{h}_1^\top \boldsymbol{\omega}) - 2\cos(\mathbf{h}_2^\top \boldsymbol{\omega})\}$ is estimating a spectral mean $M(\psi) = 0$ of zero under H_0. Guan et al. (2004) proposed subsampling for setting critical values for this test statistic, but we may also examine the effectiveness of the proposed HFDB method as well as FDWB from Ng et al. (2021). In testing, both FDWB and HFDB versions of this test statistic are computed as in (4.8) and (4.9), respectively, upon applying $\psi(\boldsymbol{\omega}) \equiv \{2\cos(\mathbf{h}_1^\top \boldsymbol{\omega}) - 2\cos(\mathbf{h}_2^\top \boldsymbol{\omega})\}$; these bootstrap statistics are then centered to have mean zero which mimics how the original-data test statistic $H_n(\psi) \equiv \sqrt{n}\widehat{M}_n(\psi)$ behaves under isotropy H_0 with $M(\psi) = 0$.

For purposes of simulating spatial data to examine size control and power in testing, we use a mean zero Gaussian process with a spherical covariance function,

$$\gamma(\mathbf{h}) \equiv \begin{cases} \sigma^2\left(1 - \frac{3r}{2\phi} + \frac{r^3}{2\phi^3}\right) + \eta\mathbb{I}\{\mathbf{h} = \mathbf{0}\} & \text{if } 0 \le r \le \phi, \\ \eta\mathbb{I}\{\mathbf{h} = \mathbf{0}\} & \text{otherwise,} \end{cases} \tag{5.10}$$

where σ^2 is the partial sill parameter, ϕ is the range parameter, η is the nugget effect, and $r \equiv \sqrt{\mathbf{h}^\top B \mathbf{h}}$ is a distance related to a matrix B, described next, as geometric anisotropy transformation. Given an anisotropy angle τ_A and anisotropy ratio τ_R, define the rotation matrix R and shrinking matrix T as

$$R \equiv \begin{bmatrix} \cos(\tau_A) & \sin(\tau_A) \\ -\sin(\tau_A) & \cos(\tau_A) \end{bmatrix} \text{ and } T \equiv \begin{bmatrix} 1 & 0 \\ 0 & \tau_R \end{bmatrix},$$

then we may set $B \equiv R'T'TR$ is a 2×2 positive definite matrix representing a geometric anisotropy transformation. A random field with spherical covariance function as in (5.10) is called generally anisotropic unless $\tau_R = 1$ holds, which corresponds to the isotropic case. We consider model parameters $(\eta, \sigma^2, \phi, \tau_A, \tau_R) = (2, 3, 4, 0, \tau_R)$ for different anisotropy ratios τ_R to generate mean-zero Gaussian data $G(\cdot)$, following Guan et al. (2004) and Ng et al. (2021). To consider a non-Gaussian process, we generate a Gaussian random field as above, and define observations as $Z(\mathbf{s}) = G(\mathbf{s}) + 0.15\big(G(\mathbf{s})^2 - E[G(\mathbf{s})^2]\big)$. This transformation preserves the process second-order structure, while inducing nonzero fourth-order cumulants (i.e., $\sigma_2^2 > 0$) in the distribution of test statistics, which represents a situation where differences between FDWB, HFDB, and spatial subsampling can become most apparent.

Table 2: Rejection rates of nominal 5% spatial isotropy test (isotropy if $\tau_R = 1$ here) with Subsampling (Sub), FDWB, and HFDB calibrations over Gaussian and non-Gaussian data.

Gaussian

τ_R	Sub	FDWB	HFDB
1	0.030	0.044	0.044
1.1	0.167	0.195	0.195
1.2	0.520	0.541	0.541
1.3	0.823	0.819	0.819
1.4	0.964	0.976	0.976
1.5	0.997	1	1

non-Gaussian

τ_R	Sub	HFDB
1	0.024	0.055
1.2	0.149	0.260
1.4	0.534	0.683
1.6	0.857	0.931
1.8	0.962	0.989
2	0.993	0.997

Table 2 displays empirical rejection probabilities (based on 1000 simulations) for the Gaussian and non-Gaussian processes, respectively, based on sample sizes of 50×50 with a nominal testing level of 5%; similar results with 10% nominal level appear in the Supplementary Materials. We have used block sizes of 7×7 for the Gaussian process, as in Ng et al. (2021), and 11×11 with bandwidth $(\delta_1, \delta_2) = (0.15, 0.15)$ for illustration. Both FDWB and HFDB perform similarly for Gaussian processes, as expected. In particular, both maintain size close to the nominal level of 5% when the null hypothesis of isotropy is true (i.e., $\tau_R = 1$), and both show increasing power as τ_R deviates from 1, outperforming spatial subsampling in both size control and power. However, under non-Gaussianity, FDWB largely fails to maintain size (rejection rate of 0.114 for $\tau_R = 1$) to the extent that of being unsuitable for power comparison and is excluded in Table 2 for this case. That is, FDWB exhibits inflated rejections and a lack of control over the Type I error. In contrast, both HFDB and spatial subsampling remain effective under non-Gaussianity, with HFDB showing some power advantages over subsampling as the anisotropy ratio increases.

6. Concluding Remarks

The proposed spatial resampling method, called Hybrid Frequency Domain Bootstrap (HFDB), combines two resampling approaches in the form of subsampling and bootstrap in order to validly approximation the distribution of spatial spectral mean statistics. Spectral means are fundamental spatial parameters, yet spectral statistics have complicated distributions owing to complex variances that are difficult to estimate. Previous bootstrap methods, such as the FDWB proposed by Ng et al. (2021), rely on specific distributional assumptions and can fail to provide valid distributional approximations for non-Gaussian spatial data, due to issues in correctly capturing the variances of spectral statistics for such data. In contrast, the HFDB overcomes these limitations by incorporating a scaling adjustment from spatial subsampling to correct the spread of bootstrap approximations in the frequency domain. This leads to more accurate and general estimation of the sampling distribution of spatial spectral mean statistic, as suggested by theory and numerical results in Sections 3-5.

While we have focused on gridded spatial data here, the general HFDB approach of approximating the complicated distribution of spectral mean statistics, by combining periodogram resampling with subsampling variance corrections, can potentially be extended to inference about spatial processes with irregular sampling locations. However, several new challenges arise in this setting that are not present in the gridded spatial case. Firstly, due to the irregular pattern of sampling locations, the spatial periodogram can have a multiplicative bias (i.e., estimating $Kf(\boldsymbol{\omega})$ rather than the true spectral density $f(\boldsymbol{\omega})$ for some $K \neq 1$, cf. Bandyopadhyay and Lahiri, 2010). As a consequence, spectral mean estimators also have multiplicative biases along with variance expressions/corrections that can change with the pattern of spatial locations. Additionally, spectral mean estimators based on irregularly located spatial data also require defining or specifying a grid of frequency spacings to evaluate discrete integrals. This aspect is less natural than for spatial lattice data and can create non-trivial additive bias for spatial spectral means (i.e., non-vanishing bias in large samples); see Subba Rao (2018) or Zhang (2024). A modified version of HFDB could potentially accommodate such biases through bias adjustments (as initially explored here) or appropriate frequency grid choices, but requires further study. Finally, general distributional theory for spectral means under non-regular locations remains a difficult and open problem. While spectral mean statistics can have normal limits, even for stochastically located spatial data, current results are mainly restricted to uniform sampling locations (cf. Subba Rao, 2018, Zhang, 2024), whereby biases (related to periodogram bias above) and variances have somewhat simplified expressions. HFDB developments for irregular spatial data could provide useful distribution approximations, though require more investigation.

Appendix

For notational simplicity, we shall use b rather than b_n in the following. The proofs of Theorem 3.1 and Theorem 4.1 involve several technical Lemmas 1-3 provided below, which are established in Supplementary Materials. Define $G^*(\boldsymbol{\omega}_{\mathbf{j},n}) := \widehat{f}_n(\boldsymbol{\omega}_{\mathbf{j},n})U^*_{\mathbf{j}}$, where $U^*_{\mathbf{j}}$s are i.i.d standard exponential drawn using the exponential resampling mechanism.

Lemma 1. *Suppose Assumptions 1-3 hold with* $H_n(\psi) \equiv n^{1/2}\{\widehat{M}_n(\psi) - M(\psi)\} \xrightarrow{D} \mathcal{N}(0,\sigma^2)$ *and* $\widehat{M}_n(\psi), M(\psi)$, $\sigma^2 \equiv \sigma^2(\psi)$ *from Section 2.2-2.3. Then, if subsample size* $b \equiv n_1^{(b)} n_2^{(b)}$ *satisfies* $1/n_k^{(b)} + n_k^{-1} n_k^{(b)} \to 0$ *for* $k = 1,2$ *as* $n \equiv n_1 n_2 \to \infty$,

(i) $\sup_{x\in\mathbb{R}} \left| L^{-1}\sum_{l=1}^{L} \mathbb{I}\{b^{1/2}(\widehat{M}^{(\ell)}_{\text{sub}}(\psi) - M(\psi)) \le x\} - P(H_n(\psi) \le x)\right| \xrightarrow{P} 0$;

(ii) $\sup_{x\in\mathbb{R}} \left| L^{-1}\sum_{l=1}^{L} \mathbb{I}\{b^{1/2}(\widehat{M}^{(\ell)}_{\text{sub}}(\psi) - \widetilde{M}_n(\psi)) \le x\} - P(H_n(\psi) \le x)\right| \xrightarrow{P} 0$;

(iii) $b^{1/2}(\widetilde{M}_n(\psi) - M(\psi)) \xrightarrow{P} 0$; *(iv)* $L^{-1}\sum_{l=1}^{L} b(\widehat{M}^{(\ell)}_{\text{sub}}(\psi) - M(\psi))^2 \xrightarrow{P} \sigma^2(\psi)$;

and (v) $L^{-1}\sum_{l=1}^{L} b(\widehat{M}^{(\ell)}_{\text{sub}}(\psi) - \widetilde{M}_n(\psi))^2 \xrightarrow{P} \sigma^2(\psi)$,

with subsample quantities $\widehat{M}^{(\ell)}_{\text{sub}}(\psi)$, $\widetilde{M}_n(\psi)$ *from Section 3.1.*

Lemma 2. *Suppose Assumptions 1-4 hold with* $\psi : \Pi^2 \to \mathbf{R}$ *of bounded variation. Then, if the subsample size* $b \equiv n_1^{(b)} n_2^{(b)}$ *satisfies* $1/n_k^{(b)} + n_k^{-1} n_k^{(b)} \to 0$ *for* $k = 1,2$ *as* $n \equiv n_1 n_2 \to \infty$,

$$4\pi^2 b^{-1} \sum_{\mathbf{j}\in\mathcal{J}_b} \psi(\boldsymbol{\omega}_{\mathbf{j},b}) L^{-1} \sum_{\ell=1}^{L} \left(\mathcal{I}^{(\ell)}_{\text{sub}}(\boldsymbol{\omega}_{\mathbf{j},b}) - \widetilde{\mathcal{I}}_n(\boldsymbol{\omega}_{\mathbf{j},b})\right)^2 \xrightarrow{P} \int_{\Pi^2} \psi(\boldsymbol{\omega}) f^2(\boldsymbol{\omega}) d\boldsymbol{\omega}.$$

Lemma 3. *Under Lemma 2 conditions with* $Q^*_{FDWB,n}(\psi)$ *from Section 4, as* $n \to \infty$,

(i) $\text{Var}_*\{Q^*_{FDWB,n}(\psi)\} \xrightarrow{P} \sigma_1^2(\psi)$; *(ii)* $\sup_{x\in\mathbb{R}} \left|P_*(Q^*_{FDWB,n}(\psi) \le x) - \Phi(x/\sigma_1(\psi))\right| \xrightarrow{P} 0$, *where* Var_*, P_* *denote variance and probability induced by resampling, and* $\Phi(\cdot)$ *is the standard normal distribution function.*

Proof of Theorem 3.1

Using Lemma 2, we have $\widehat{\sigma}^2_{1,n}(\psi) \xrightarrow{P} \sigma_1^2(\psi)$. Since, $\psi(\cdot)$ is of bounded variation, so is $\psi(\boldsymbol{\omega})(\psi(\boldsymbol{\omega}) + \psi(-\boldsymbol{\omega}))$. Using Slutsky's theorem and Lemma 1(v) we have $\widehat{\sigma}^2_{2,n}(\psi) = \widehat{\sigma}^2_n(\psi) - \widehat{\sigma}^2_{1,n}(\psi) \xrightarrow{P} \sigma^2(\psi) - \sigma_1^2(\psi) = \sigma_2^2(\psi)$. The statement of Theorem 3.1 now follows. $\square$

Proof of Theorem 4.1

Part (a) follows by applying Lemma 3(i) and Slutsky's theorem to give $\mathrm{Var}_*\{Q^*_{FDWB,n}(\psi)\} + \widehat{\sigma}^2_{2,n}(\psi) \xrightarrow{P} \sigma^2(\psi)$. To prove the consistency of the HFDB distribution in part (b), consider an arbitrary sequence $\{n_m\}$ of $\{n\}$. Then, from Lemma 3 and Theorem 3.1, there exists a further subsequence $\{n_{m_k}\}$ of $\{n_m\}$ such that almost sure convergence holds as

$$\sup_{x\in\mathbb{R}} \left| P_*(Q^*_{FDWB,n_{m_k}}(\psi) \le x) - \Phi(x/\sigma_1(\psi)) \right| \xrightarrow{a.s.} 0; \quad \mathrm{Var}_*\{Q^*_{FDWB,n_{m_k}}(\psi)\} \xrightarrow{a.s.} \sigma_1^2(\psi);$$

and $\mathrm{Var}_*\{Q^*_{FDWB,n_{m_k}}(\psi)\} + \widehat{\sigma}^2_{2,n_{m_k}}(\psi) \xrightarrow{a.s} \sigma^2(\psi)$ as $n_{m_k} \to \infty$. Using these facts with the HFDB definition, along the subsequence $\{n_{m_k}\}$, we have $H^*_{HFDB,n_{m_k}}(\psi) \xrightarrow{D} \mathcal{N}(0, \sigma^2(\psi))$ by Slutsky's theorem, or equivalently $\sup_{x\in\mathbb{R}} |P_*(H^*_{HFDB,n_{m_k}}(\psi) \le x) - \Phi(x/\sigma(\psi))| \xrightarrow{a.s} 0$ as $n_{m_k} \to \infty$. Since the choice of the sub-sequence was arbitrary, we have

$$\sup_{x\in\mathbb{R}} \left| P_*(H^*_{HFDB,n}(\psi) \le x) - \Phi(x/\sigma(\psi)) \right| \xrightarrow{P} 0 \text{ as } n \to \infty.$$

Now using $\sup_{x\in\mathbb{R}} |P(H_n(\psi) \le x) - \Phi(x/\sigma(\psi))| = o_P(1)$ completes the proof. □

Supplementary Materials

Supplementary Materials present additional finite sample simulation results in support of the proposed method, along with proof details of technical lemmas. Figures and tables presented in this paper are generated using code available in the GitHub repository: HFDB git.

Acknowledgments

The authors are grateful to the Associate Editor, and the two reviewers for thoughtful comments that substantially improved the manuscript. The authors are also thankful to

NSF for the NSF ACCESS MTH250064 allocation and for support by NSF DMS-2514857 (Bera and Bandyopadhyay) and 2515719 (Nordman).

References

Anselin, L. (1988). *Spatial econometrics: methods and models*, Volume 4. Springer Science & Business Media.

Bandyopadhyay, S., C. Jentsch, and S. S. Rao (2017). A spectral domain test for stationarity of spatio-temporal data. *Journal of Time Series Analysis 38*(2), 326–351.

Bandyopadhyay, S. and S. N. Lahiri (2010). Asymptotic properties of Discrete Fourier transforms for spatial data. *Sankhya 71*, 221–259.

Bandyopadhyay, S., S. N. Lahiri, and D. J. Nordman (2015). A frequency domain empirical likelihood method for irregularly spaced spatial data. *The Annals of Statistics 43*(2), 519–545.

Bandyopadhyay, S. and S. S. Rao (2016). A test for stationarity for irregularly spaced spatial data. *Journal of the Royal Statistical Society: Series B 79*(1), 95–123.

Beran, J. (1992). A goodness-of-fit test for time series with long range dependence. *Journal of the Royal Statistical Society Series B: Statistical Methodology 54*(3), 749–760.

Besag, J. E. (1974). Spatial interaction and the statistical analysis of lattice systems (with discussion). *Journal of the Royal Statistical Society, Series B 35*, 192–236.

Brillinger, D. R. (2001). *Time Series*. Society for Industrial and Applied Mathematics, Philadelphia, PA.

Caragea, P. C. and M. S. Kaiser (2009). Autologistic models with interpretable parameters. *Journal of agricultural, biological, and environmental statistics 14*(3), 281–300.

Cressie, N. A. C. (1993). *Statistics for Spatial Data* (revised ed.). Wiley.

Crujeiras, R. M. and R. Fernandez-Casal (2010). On the estimation of the spectral density for continuous spatial processes. *Statistics 44*(6), 587–600.

Dahlhaus, R. (1985). Asymptotic normality of spectral estimates. *Journal of Multivariate Analysis 16*(3), 412–431.

Dahlhaus, R. and D. Janas (1996). A frequency domain bootstrap for ratio statistics in time series analysis. *The Annals of Statistics 24*(5), 1934–1963.

Datta, A., S. Banerjee, A. O. Finley, and A. E. Gelfand (2016). On nearest-neighbor gaussian process models for massive spatial data. *Wiley Interdisciplinary Reviews: Computational Statistics 8*(5), 162–171.

Davison, A. C. and D. V. Hinkley (1997). *Bootstrap methods and their application*. Number 1. Cambridge university press.

Fuentes, M. (2006). Testing for separability of spatial-temporal covariance functions. *Journal of Statistical Planning and Inference 136*, 447–466.

Fuentes, M. (2007). Approximate likelihood for large irregularly spaced spatial data. *Journal of the American Statistical Association 102*, 321–331.

Guan, Y., M. Sherman, and J. A. Calvin (2004). A nonparametric test for spatial isotropy using subsampling. *Journal of the American Statistical Association 99*(467), 810–821.

Guyon, X. (1995). *Random fields on a network: modeling, statistics, and applications*. Springer Science & Business Media.

Hall, P., N. I. Fisher, and B. Hoffman (1994). On the nonparametric estimation of covariance functions. *Annals of Statistics 22*, 2115–2134.

Hardouin, C. and J.-F. Yao (2008). Multi-parameter automodels and their applications. *Biometrika 95*(2), 335–349.

Im, H. K., M. L. Stein, and Z. Zhu (2007). Semiparametric estimation of spectral density with irregular observations. *Journal of the American Statistical Association 102*(478), 726–735.

Jentsch, C. and J.-P. Kreiss (2010). The multiple hybrid bootstrap—resampling multivariate linear processes. *Journal of Multivariate Analysis 101*(10), 2320–2345.

Kaiser, M. S., N. Cressie, and J. Lee (2002). Spatial mixture models based on exponential family conditional distributions. *Statistica Sinica*, 449–474.

Kreiss, J.-P. and S. N. Lahiri (2012). Bootstrap methods for time series. In *Handbook of statistics*, Volume 30, pp. 3–26. Elsevier.

Kreiss, J.-P. and E. Paparoditis (2003). Autoregressive-aided periodogram bootstrap for timeseries. *The Annals of Statistics 31*(6), 1923–1955.

Kreiss, J.-P. and E. Paparoditis (2012). The hybrid wild bootstrap for time series. *Journal of the American Statistical Association 107*(499), 1073–1084.

Kreiss, J.-P. and E. Paparoditis (2023). Bootstrapping whittle estimators. *Biometrika 110*(2), 499–518.

Kreiss, J.-P., E. Paparoditis, and D. N. Politis (2011). On the range of validity of the autoregressive sieve bootstrap. *Annals of Statistics*, 2103–2130.

Lahiri, S., K. Furukawa, and Y.-D. Lee (2007). A nonparametric plug-in rule for selecting optimal block lengths for block bootstrap methods. *Statistical methodology 4*(3), 292–321.

Lahiri, S. N. (2003a). Central limit theorems for weighted sums of a spatial process under a class of stochastic and fixed designs. *Sankhyā: The Indian Journal of Statistics*, 356–388.

Lahiri, S. N. (2003b). *Resampling methods for dependent data*. Springer Science & Business Media.

Li, W. and A. McLeod (1986). Fractional time series differencing. *Biometrika 73*, 217–221.

Ljung, G. M. and G. E. Box (1978). On a measure of lack of fit in time series models. *Biometrika 65*(2), 297–303.

Matsuda, Y. and Y. Yajima (2009). Fourier analysis of irregularly spaced data on rd. *Journal of the Royal Statistical Society: Series B 71*(1), 191–217.

Meyer, M., E. Paparoditis, and J.-P. Kreiss (2020). Extending the validity of frequency domain bootstrap methods to general stationary processes. *The Annals of Statistics 48*(4), 2404–2427.

Milhøj, A. (1981). A test of fit in time series models. *Biometrika 68*(1), 177–187.

Ng, W. L., C. Y. Yau, and X. Chen (2021). Frequency domain bootstrap methods for random fields. *Electronic Journal of Statistics 15*(2), 6586–6632.

Nordman, D. J. and S. N. Lahiri (2004). On optimal spatial subsample size for variance estimation. *The Annals of Statistics 32*(5), 1981–2027.

Nordman, D. J. and S. N. Lahiri (2006). A frequency domain empirical likelihood for short-and long-range dependence. *The Annals of Statistics*, 3019–3050.

Paparoditis, E. (2000). Spectral density based goodness-of-fit tests for time series models. *Scandinavian Journal of Statistics 27*(1), 143–176.

Parzen, E. (1957). On consistent estimates of the spectrum of a stationary time series. *The Annals of Mathematical Statistics*, 329–348.

Politis, D. N. and T. S. McElroy (2019). *Time series: A first course with bootstrap starter.* CRC Press.

Politis, D. N., J. P. Romano, and M. Wolf (1999). *Subsampling.* Springer Science & Business Media.

Sherman, M. (1996). Variance estimation for statistics computed from spatial lattice data. *Journal of the Royal Statistical Society Series B: Statistical Methodology 58*(3), 509–523.

Sherman, M. (1998). Efficiency and robustness in subsampling for dependent data. *Journal of statistical planning and inference 75*(1), 133–146.

Sherman, M. and E. Carlstein (1994). Nonparametric estimation of the moments of a general statistic computed from spatial data. *Journal of the American Statistical Association 89*(426), 496–500.

Stein, M. L. (1999). *Interpolation of spatial data: some theory for kriging.* Springer Science & Business Media.

Subba Rao, S. (2018). Statistical inference for spatial statistics defined in the fourier domain. *The Annals of Statistics 46*(2), 469–499.

Taniguchi, M. (1979). On estimation of parameters of gaussian stationary processes. *Journal of Applied Probability 16*(3), 575–591.

Tjøstheim, D. (1978). Statistical spatial series modelling. *Advances in Applied Probability 10*(1), 130–154.

Van Hala, M., S. Bandyopadhyay, S. N. Lahiri, and D. J. Nordman (2017). On the non-standard distribution of empirical likelihood estimators with spatial data. *Journal of Statistical Planning and Inference 187*, 109–114.

Van Hala, M., S. Bandyopadhyay, S. N. Lahiri, and D. J. Nordman (2020). A general frequency domain method for assessing spatial covariance structures. *Bernoulli 26*(4), 2463–2487.

Weller, Z. D. and J. A. Hoeting (2020). A nonparametric spectral domain test of spatial isotropy. *Journal of statistical planning and inference 204*, 177–186.

Yu, H., M. S. Kaiser, and D. J. Nordman (2023). A subsampling perspective for extending the validity of state-of-the-art bootstraps in the frequency domain. *Biometrika*, asad006.

Zhang, S. (2024). Statistical analysis of irregularly spaced spatial data in frequency domain. *Journal of Time Series Analysis 45*(5), 714–738.

Department of Applied Mathematics and Statistics,

Colorado School of Mines, Golden, CO 80401, USA.

E-mail: (berasouvick@mines.edu)

Department of Applied Mathematics and Statistics,

Colorado School of Mines, Golden, CO 80401, USA.

E-mail: (sbandyopadhyay@mines.edu)

Department of Statistics,

Iowa State University, Ames, IA 50011, USA.

E-mail: (dnordman@iastate.edu)